

Introduction

This book¹ presents original mathematical models of thermal and phase-transformation stresses in composite materials with three components. These stresses originate during a cooling process. In contrast to mathematical models of these stresses in two-component materials, which are determined in the first volume [1], the three-component materials consist of an isotropic matrix and isotropic ellipsoidal inclusions with an isotropic ellipsoidal envelope on the inclusion surface.

The thermal stresses are a consequence of different thermal expansion coefficients of the matrix, the envelope and the inclusion. The phase-transformation stresses are a consequence of different dimensions of cubic crystalline lattices (see Section 2.3), which are transformed in the material components.

The mathematical models are determined for a suitable three-component model system. This infinite periodic matrix-envelope-inclusion model system corresponds to real isotropic matrix-envelope-inclusion composites, which consist of

- isotropic precipitates with an isotropic continuous component on their surfaces, distributed in isotropic crystalline grains,
- isotropic crystalline grains with and without an isotropic continuous component (E) on their surfaces, and the crystalline grains exhibit identical or different material properties, i.e., the real three-component material consists of the crystalline grains $A + E$, A or $A + E$, B , respectively, where A , B represent crystalline grains with different material properties.

The precipitates, the continuous component on their surfaces and the crystalline grains of a real composite represent the inclusion, envelope and matrix of the matrix-envelope-inclusion system, respectively. Similarly, the crystalline grains $A + E$ and A , B of a real composite represent the inclusion with the envelope and the matrix, respectively.

¹This book was supported by the Slovak scientific grant agency VEGA 2/0069/24.

Mathematical and computational models of phenomena in infinite periodic model material systems are determined within a representative volume element with such geometric characteristics to correspond to microstructural characteristics of the model material system. Due to the infinity and periodicity, the mathematical and computational models, which are determined for a certain representative volume element, are valid for any representative volume element. Infinite matrixes are used due to simplicity of mathematical solutions for material components (e.g., precipitates, pores). The material components are small in comparison with macroscopic material samples or macroscopic structural elements, and then the solutions are acceptable in spite of this simplification [2]. In case of the matrix-envelope-inclusion system, this volume element is represented by a cubic cell with a central ellipsoidal inclusion and the ellipsoidal envelope on the inclusion surface.

The mathematical models results from fundamental equations of mechanics of an elastic continuum (i.e., Cauchy's and equilibrium equations, Hooke's law), with respect to its shape, loading, mechanical constraints and the principle of minimum potential energy. The stresses are derived within a suitable coordinate system, which is required to correspond to a shape of the ellipsoidal inclusion and the ellipsoidal envelope. Consequently, the fundamental equations results in different mathematical solutions for the stresses in components of the matrix-envelope-inclusion system. Additionally, the mathematical solutions are determined with respect to mechanical constraints, i.e., mathematical boundary conditions, for the ellipsoidal inclusion, the ellipsoidal envelope and the cell matrix. Due to these different mathematical solutions, the principle of minimum potential energy is required to be considered.

Additionally, the stress fields, i.e., the thermal and phase-transformation stresses, in neighbouring cells are mutually affected. The stress field in a certain cell is then affected by those in neighbouring cells, and vice versa. This effect is determined by the superposition method of mechanics of a solid continuum [3].

The mathematical models for the three-component materials are applicable to those for the micro-/macro-strengthening and crack formation, which are determined in the first volume [1].

Matrix-Envelope-Inclusion Composite

1.1 Model System

Figure 1.1 shows a model system, corresponding to real matrix-envelope-inclusion composites, which is considered within the mathematical models of the thermal and phase-transformation stresses.

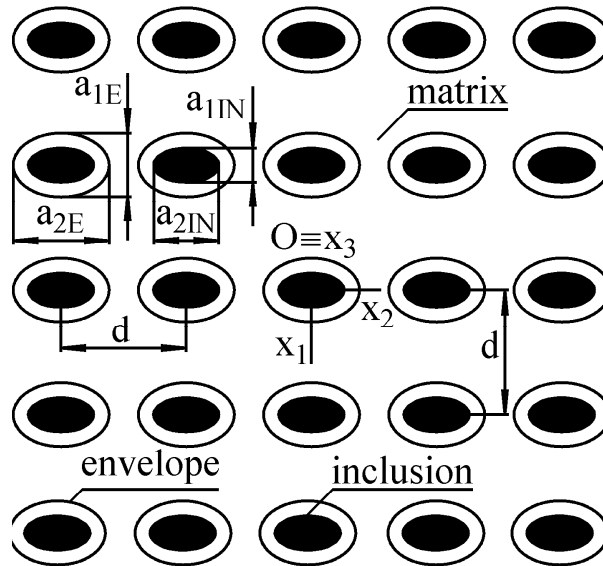


Figure 1.1: The matrix-envelope-inclusion system with an infinite isotropic matrix with isotropic ellipsoidal envelopes on a surface of isotropic ellipsoidal inclusions with the dimensions a_{1q} , a_{2q} , a_{3q} ($q = IN, E$) and the inter-inclusion distance d along the axes x_1 , x_2 , x_3 of the Cartesian system ($Ox_1x_2x_3$), respectively, where O represents a centre of the ellipsoidal inclusion. The subscript $q = IN$ and $q = E$ is related to the inclusion and envelope, respectively.

This model system consists of an infinite isotropic matrix with isotropic ellipsoidal envelopes on a surface of isotropic ellipsoidal inclusions with the dimensions a_{1q} , a_{2q} , a_{3q} ($q = IN, E$) and the inter-inclusion distance d along the axes x_1 , x_2 , x_3 of the Cartesian system ($Ox_1x_2x_3$), respectively, where O

represents a centre of the ellipsoidal inclusion. The subscript $q = IN$ and $q = E$ is related to the inclusion and envelope, respectively.

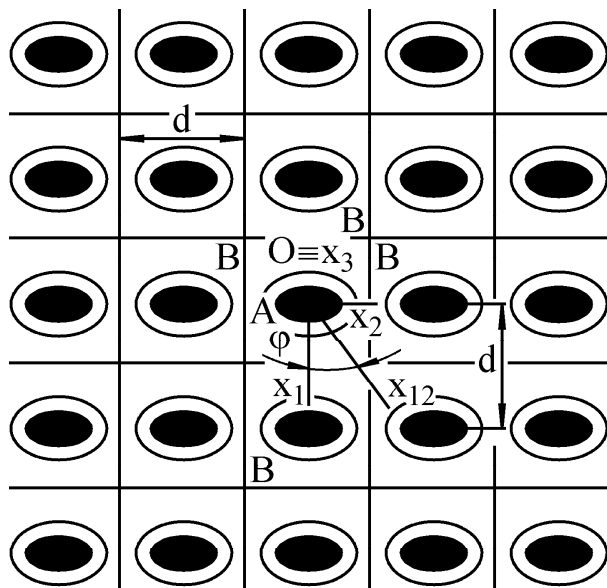


Figure 1.2: The cubic cells with the dimension d along the axes x_1, x_2, x_3 of the Cartesian system $(Ox_1x_2x_3)$ and with the plane $x_{12}x_3$, where O represents a centre of the ellipsoidal inclusion, and $x_{12} \subset x_1x_2, x_{12}x_3 \perp x_1x_2$.

The thermal and phase-transformation stresses are determined in the cubic cells with the dimension d along the axes x_1, x_2, x_3 and with central ellipsoidal inclusions (see Figure 1.2). Due to the infinite matrix, the thermal and phase-transformation stresses, which are determined for one of the cubic cells, are identical with those, which are determined for any of the cubic cells. With regard to the volume $V_{IN} = 4\pi a_1 a_2 a_3$ [4] and $V_C = d^3$ of the ellipsoidal inclusion and the cubic cell, the inter-inclusion distance d as a function of the inclusion volume fraction v_{IN} is derived as

$$v_{IN} = \frac{V_{IN}}{V_C} = \frac{4\pi a_{1IN} a_{2IN} a_{3IN}}{3d^3} \in \left(0, \frac{\pi}{6}\right), \quad d = \left(\frac{4\pi a_{1IN} a_{2IN} a_{3IN}}{3v_{IN}}\right)^{1/3}, \quad (1.1)$$

where the value $v_{INmax} = \pi/6$ results from the condition $a_{iIN} \rightarrow a_{iE} \rightarrow d/2$ ($i=1,2,3$). Accordingly, the thermal and phase-transformation stresses are functions of the material parameters a_{iq} ($i=1,2,3; q=IN,E$), v_{IN} , d .

1.2 Coordinate System

The thermal and phase-transformation stresses are determined by the spherical coordinates (r, φ, ν) (see Figure 1.3). The model system in Figures (1.1), (1.2) is symmetric, and then these stresses are determined within the intervals $\varphi \in \langle 0, \pi/2 \rangle$, $\nu \in \langle 0, \pi/2 \rangle$.

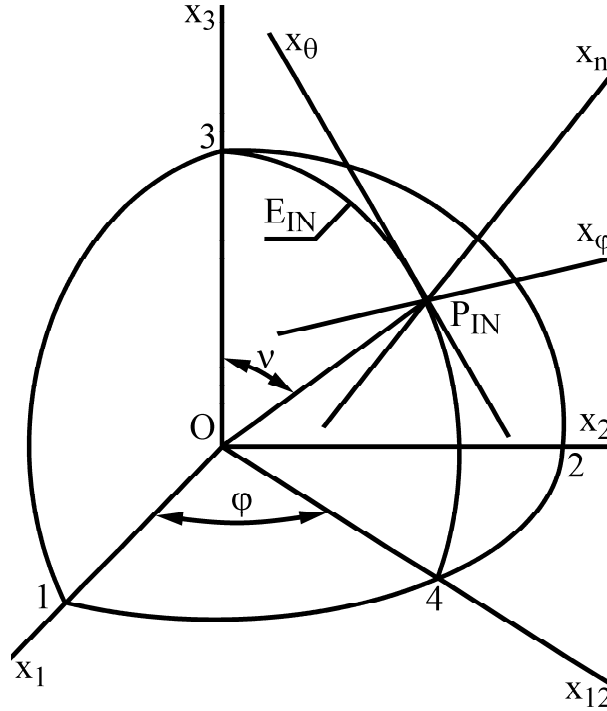


Figure 1.3: The inclusion with the centre O and with the dimensions $a_{1IN} = O1$, $a_{2IN} = O2$, $a_{3IN} = O3$ along the axes x_1 , x_2 , x_3 of the Cartesian system (O, x_1, x_2, x_3) , respectively. The point P_{IN} on the inclusion surface is defined by $\varphi, \nu \in \langle 0, \pi/2 \rangle$, and $(P_{IN}, x_n, x_\varphi, x_\nu)$ is a Cartesian system at the point P_{IN} , where $P_{IN} \subset E_{IN}$. The axes x_n and x_ν represents a normal and a tangent of the ellipse E_{IN} at the point P_{IN} , respectively. Due to clarity of Figure 1.3 the ellipsoidal envelope in Figures 1.1, 1.2 is not depicted in Figure 1.3.

Figure 1.3 shows the ellipsoidal inclusion for $\varphi, \nu \in \langle 0, \pi/2 \rangle$ with the centre O and with the dimensions $a_{1IN} = O1$, $a_{2IN} = O2$, $a_{3IN} = O3$ along the axes x_1 , x_2 , x_3 of the Cartesian system (O, x_1, x_2, x_3) (see Figures (1.1), (1.2)), respectively. Due to clarity of Figure 1.3 the ellipsoidal envelope in Figures 1.1, 1.2 is not depicted in Figure 1.3. Finally, $(P_{IN}, x_n, x_\varphi, x_\nu)$ is a Cartesian system at the point P_{IN} , where the axes x_n and x_ν represents a normal and a tangent of the ellipse E_{IN} at the point P_{IN} , respectively, $x_{12}x_3 \perp x_1x_2$, $(x_{12} \subset x_1x_2, x_\varphi \perp x_{12}$.

Figure 1.4 shows the cross section $O789$ of the cubic cell in the plane $x_{12}x_3$ (see Figures 1.2, 1.3). The angle $\nu \in \langle 0, \pi/2 \rangle$ defines a position of the point

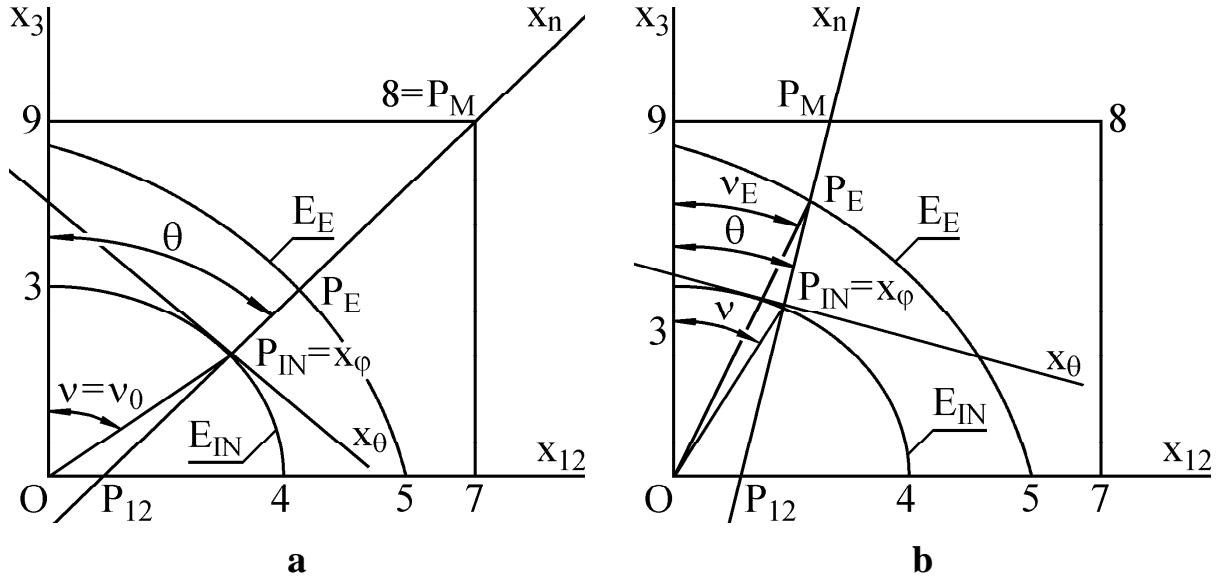
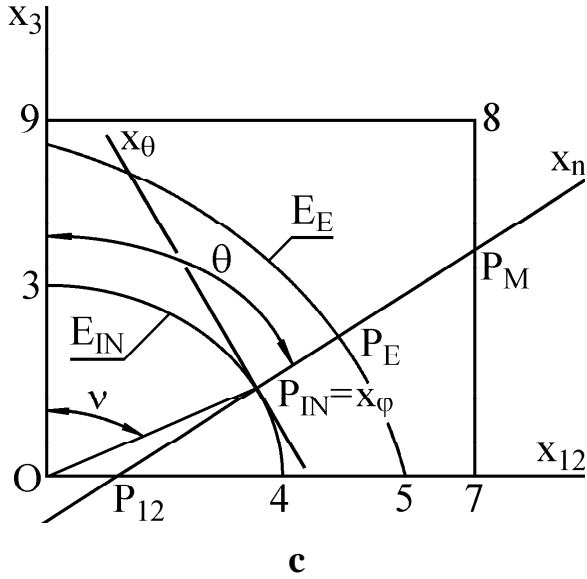


Figure 1.4: The angle $v \in \langle 0, \pi/2 \rangle$ defines a position of the point P_{IN} with the Cartesian system $(P_{IN}, x_n, x_\phi, x_v)$ (see Figure 1.3) for (a) $v = v_0$, (b) $v \in \langle 0, v_0 \rangle$, (c) $v \in (v_0, \pi/2 \rangle$, where v_0 represents a root of Equation (1.6). The points P_{12}, P_M represent intersections of the normal x_n with $O789$, where $O789$ is a cross section of the cubic cell in the plane $x_{12}x_3$ (see Figures 1.2, 1.3). The angle $\theta = \angle(x_n, x_3)$ is given by Equation (1.2). Due to clarity of Figure 1.4, the angle $v_E = \angle(OP_E, x_3)$ (see Equation (1.2)) is depicted in Figure 1.4b only.



P_{IN} with the Cartesian system $(P_{IN}, x_n, x_\phi, x_v)$ (see Figure 1.3) for $v = v_0$ (see Figure 1.4a), $v \in \langle 0, v_0 \rangle$ (see Figure 1.4b), $v \in (v_0, \pi/2 \rangle$ (see Figure 1.4c). The points P_{12}, P_M represent intersections of the normal x_n with $O789$. Due to clarity of Figure 1.4, the angle $v_E = \angle(OP_E, x_3)$ (see Equation (1.2)) is depicted in Figure 1.4b only. The angles $v_E = \angle(OP_E, x_3)$, $\theta = \angle(x_n, x_3)$ (see Figure 1.4), along with the derivative $\partial/\partial\theta$, have the forms [1]

$$\sin v_E = \frac{a_{1E} a_{3IN} \tan v}{\sqrt{(a_{1IN} a_{3E})^2 + (a_{1E} a_{3IN} \tan v)^2}},$$

$$\begin{aligned}\cos v_E &= \frac{a_{1IN} a_{3E}}{\sqrt{(a_{1IN} a_{3E})^2 + (a_{1E} a_{3IN} \tan v)^2}}; \\ \sin \theta &= \frac{1}{\sqrt{1 + (a_{1IN} \cot v / a_{3IN})^2}}, \quad \cos \theta = \frac{1}{\sqrt{1 + (a_{3IN} \tan v / a_{1IN})^2}}, \\ \frac{\partial}{\partial \theta} &= \left(\frac{\partial \theta}{\partial v} \right)^{-1} \frac{\partial}{\partial v} = \Theta \frac{\partial}{\partial v}, \quad \Theta = \left(\frac{a_{1IN}}{a_{3IN}} \right) \left[\left(\frac{a_{3IN} \sin v}{a_{1IN}} \right)^2 + \cos^2 v \right].\end{aligned}\quad (1.2)$$

Let x_{nIN} and x_{nE} represent normals on the envelope-inclusion and envelope-matrix boundaries at the points P_{IN} and P_E , respectively. Due to the symmetry of the model system, any points P_{IN} and P_E on the envelope-inclusion and envelope-matrix boundaries (see Figure 1.4) exhibit the displacements u_{nIN} and u_{nE} along the normals x_{nIN} and x_{nE} , respectively, i.e., $u_{\varphi q} = u_{vq} = 0$ ($q = IN, E$) [5], where $u_{\varphi q}$, u_{vq} are displacements along the tangents $x_{\varphi q}$, x_{vq} , respectively.

Consequently, the mathematical models in this book can be determined provided that $u_{\varphi q} = u_{vq} = 0$ ($q = IN, E$), which results in the condition $x_n = x_{nIN} = x_{nE}$. Finally, the condition $x_n = x_{nIN} = x_{nE}$ defines relationships between the dimensions a_{iIN} and a_{iE} ($i = 1, 2, 3$), which have the forms

$$\begin{aligned}\frac{a_{1IN}^2 - a_{3IN}^2}{a_{1IN} a_{3IN}} &= \frac{a_{1E}^2 - a_{3E}^2}{a_{1E} a_{3E}}, \quad a_{1q} = a_{2q} \neq a_{3q}, \quad a_{iIN} < a_{iE}, \quad i = 1, 2, 3, \\ q &= IN, E.\end{aligned}\quad (1.3)$$

With regard to Equation (1.3), the ellipsoidal inclusion and ellipsoidal envelope are required to represent a rotational ellipsoid (a spheroid), i.e., $a_{1q} = a_{2q} \neq a_{3q}$ ($q = IN, E$).

The thermal and phase-transformation stresses, which are determined along the axes x_n , x_φ , x_θ of the Cartesian system $(P, x_n, x_\varphi, x_\theta)$, represent function of the spherical coordinates (x_n, φ, θ) for $\varphi, \theta \in \langle 0, \pi/2 \rangle$. The intervals $x_n \in \langle 0, x_{IN} \rangle$, $x_n \in \langle x_{IN}, x_E \rangle$ and $x_n \in \langle x_E, x_M \rangle$ are related to the ellipsoidal inclusion, envelope and cell matrix, respectively. Finally, we get

$$\begin{aligned}x_{IN} &= P_{12} P_{IN} = \sqrt{(a_{1IN} \sin v - x_{120})^2 + (a_{3IN} \cos v)^2}, \\ x_E &= P_{IN} P_E = \sqrt{(a_{1E} \sin v_E - a_{1IN} \sin v)^2 + (a_{3E} \cos v_E - a_{3IN} \cos v)^2}, \\ x_M &= P_E P_M = \sqrt{(x_{12M} - a_{1E} \sin v_E)^2 + (x_{3M} - a_{3E} \cos v_E)^2},\end{aligned}\quad (1.4)$$

where $\sin v_E$, $\cos v_E$ are given by Equations (1.2), and x_{120} , x_{12M} , x_{3M} are derived as [1]

$$\begin{aligned}
x_{120} &= \frac{(a_{1IN}^2 - a_{3IN}^2) \sin \nu}{a_{1IN}}, \quad \nu \in \left\langle 0, \frac{\pi}{2} \right\rangle, \\
x_{12M} &= \frac{\sin \nu}{a_{1IN}} \left(\frac{d \cos \nu}{2 a_{3IN}} + a_{1IN}^2 - a_{3IN}^2 \right), \quad \nu \in \langle 0, \nu_0 \rangle, \\
x_{12M} &= \frac{d}{2 f(\varphi) \sin \nu}, \quad \nu \in \left\langle \nu_0, \frac{\pi}{2} \right\rangle, \\
x_{3M} &= \frac{d}{2}, \quad \nu \in \langle 0, \nu_0 \rangle, \\
x_{3M} &= \frac{\cos \nu}{a_{3IN}} \left[\frac{a_{1IN} d}{2 f(\varphi) \sin \nu} + a_{3IN}^2 - a_{1IN}^2 \right], \quad \nu \in \left\langle \nu_0, \frac{\pi}{2} \right\rangle, \quad (1.5)
\end{aligned}$$

where the angle ν_0 represents a root of the following equation

$$\frac{\cos \nu_0}{a_{3IN}} \left[\frac{a_{1IN} d}{2 f(\varphi) \sin \nu_0} + a_{3IN}^2 - a_{1IN}^2 \right] - \frac{d}{2} = 0, \quad (1.6)$$

and this root is determined by a numerical method. Finally, the function $f = f(\varphi)$ in Equations (1.5), (1.6) has the form

$$f(\varphi) = \cos \varphi, \quad \varphi \in \left\langle 0, \frac{\pi}{4} \right\rangle; \quad f(\varphi) = \sin \varphi, \quad \varphi \in \left\langle \frac{\pi}{4}, \frac{\pi}{2} \right\rangle. \quad (1.7)$$

Mechanics of Elastic Solid Continuum

2.1 Fundamental Equations

Due to the symmetry of the model system (see Figure 1.1), any point P of the normal x_n exhibits the displacement u_n along x_n . The thermal and phase-transformation stresses are determined along the axes x_n, x_φ, x_θ of the Cartesian system $(P, x_n, x_\varphi, x_\theta)$. Fundamental equations of mechanics of a solid continuum are represented by Cauchy's equations, the equilibrium equations and Hooke's law. Cauchy's equations represent functions of strains and displacements. With respect to the normal displacement u_n , Cauchy's equations have the forms [1]

$$\varepsilon_n = \frac{\partial u_n}{\partial x_n}, \quad (2.1)$$

$$\varepsilon_\varphi = \varepsilon_\theta = \frac{u_n}{x_n}, \quad (2.2)$$

$$\varepsilon_{n\varphi} = \varepsilon_{\varphi n} = \frac{1}{x_n} \frac{\partial u_n}{\partial \varphi}, \quad (2.3)$$

$$\varepsilon_{n\theta} = \varepsilon_{\theta n} = \frac{\Theta}{x_n} \frac{\partial u_n}{\partial \nu}, \quad (2.4)$$

where ε_n is a normal strain along the axis x_n , and Θ is given by Equation (1.2). Consequently, ε_φ and ε_θ are tangential strains along the axes x_φ and x_θ , respectively. Finally, $\varepsilon_{n\varphi}$, $\varepsilon_{n\theta}$ and $\varepsilon_{\varphi n}$, $\varepsilon_{\theta n}$ represent shear strains along the axes x_n and x_φ, x_θ , respectively. Due to $u_\varphi = u_\nu = 0$, we get $\varepsilon_{\varphi\nu} = \varepsilon_{\nu\varphi} = 0$, where u_φ, u_ν are displacements along the axes x_φ, x_ν , respectively, and $\varepsilon_{\varphi\nu}$ is a shear strain. The equilibrium equations are derived as [1]

$$2\sigma_n - \sigma_\varphi - \sigma_\nu + x_n \frac{\partial \sigma_n}{\partial x_n} + \frac{\partial \sigma_{n\varphi}}{\partial \varphi} + \Theta \frac{\partial \sigma_{n\theta}}{\partial \nu} = 0, \quad (2.5)$$

$$\frac{\partial \sigma_\varphi}{\partial \varphi} + 3\sigma_{n\varphi} + x_n \frac{\partial \sigma_{n\varphi}}{\partial x_n} = 0, \quad (2.6)$$

$$\Theta \frac{\partial \sigma_\theta}{\partial \nu} + 3\sigma_{n\theta} + x_n \frac{\partial \sigma_{n\theta}}{\partial x_n} = 0, \quad (2.7)$$

where σ_n is a normal stress along the axis x_n . Consequently, σ_φ and σ_θ are tangential stresses along the axes x_φ and x_θ , respectively. Finally, $\sigma_{n\varphi}$, $\sigma_{n\theta}$ and $\sigma_{\varphi n}$, $\sigma_{\theta n}$ represent shear stresses along the axes x_n and x_φ , x_θ , respectively, where $\sigma_{n\varphi} = \sigma_{\varphi n}$, $\sigma_{n\theta} = \sigma_{\theta n}$. Due to $\varepsilon_{\varphi\nu} = \varepsilon_{\nu\varphi} = 0$, we get $\sigma_{\varphi\nu} = \sigma_{\nu\varphi} = 0$, where $\sigma_{\varphi\nu}$ is a shear stress. With regard to $\varepsilon_{\varphi\theta} = 0$, $\sigma_{\varphi\theta} = 0$, Hooke's law has the form

$$\varepsilon_n = s_{11}\sigma_n + s_{12}(\sigma_\varphi + \sigma_\theta), \quad (2.8)$$

$$\varepsilon_\varphi = s_{12}(\sigma_n + \sigma_\theta) + s_{11}\sigma_\varphi, \quad (2.9)$$

$$\varepsilon_\theta = s_{12}(\sigma_n + \sigma_\varphi) + s_{11}\sigma_\theta, \quad (2.10)$$

$$\varepsilon_{n\theta} = s_{44}\sigma_{n\theta}, \quad (2.11)$$

$$\varepsilon_{n\varphi} = s_{44}\sigma_{n\varphi}, \quad (2.12)$$

where s_{11} , s_{12} , s_{44} are derived as [5]

$$s_{11} = \frac{1}{E}, \quad s_{12} = -\frac{\mu}{E}, \quad s_{44} = \frac{2(1+\mu)}{E}. \quad (2.13)$$

Finally, E and μ are Young's modulus and Poisson's ratio, respectively. In case of the ellipsoidal inclusion and the cell matrix, we get $E = E_{IN}$, $\mu = \mu_{IN}$ and $E = E_M$, $\mu = \mu_M$, respectively. With regard to Equations (2.1)–(2.4), (2.8)–(2.12), we get

$$\sigma_n = (c_1 + c_2) \frac{\partial u_n}{\partial x_n} - 2c_2 \frac{u_n}{x_n}, \quad (2.14)$$

$$\sigma_\varphi = \sigma_\theta = -c_2 \frac{\partial u_n}{\partial x_n} + c_1 \frac{u_n}{x_n}, \quad (2.15)$$

$$\sigma_{n\varphi} = \frac{1}{s_{44}x_n} \frac{\partial u_n}{\partial \varphi}, \quad (2.16)$$